

Original citation:

Silva Sousa, Eduardo Henrique, Ridnour, Lisa A., Gouveia, Florêncio S., Silva da Silva, Carlos Daniel, Wink, David A., de França Lopes, Luiz Gonzaga and Sadler, P. J.. (2016) Thiol-Activated HNO release from a ruthenium antiangiogenesis complex and HIF-1 α inhibition for cancer therapy. ACS Chemical Biology, 11 (7). pp. 2057-2065.

Permanent WRAP URL:

<http://wrap.warwick.ac.uk/84849>

Copyright and reuse:

The Warwick Research Archive Portal (WRAP) makes this work of researchers of the University of Warwick available open access under the following conditions.

This article is made available under the Creative Commons Attribution 4.0 International license (CC BY 4.0) and may be reused according to the conditions of the license. For more details see: <http://creativecommons.org/licenses/by/4.0/>

A note on versions:

The version presented in WRAP is the published version, or, version of record, and may be cited as it appears here.

For more information, please contact the WRAP Team at: wrap@warwick.ac.uk

Thiol-Activated HNO Release from a Ruthenium Antiangiogenesis Complex and HIF-1 α Inhibition for Cancer Therapy

Eduardo Henrique Silva Sousa,^{*,†,§} Lisa A. Ridnour,^{||} Florêncio S. Gouveia, Jr.,[†] Carlos Daniel Silva da Silva,^{†,‡} David A. Wink,^{||} Luiz Gonzaga de França Lopes,[†] and Peter J. Sadler^{*,§}

[†]Laboratory of Bioinorganic Chemistry, Department of Organic and Inorganic Chemistry, Federal University of Ceará, Mister Hull Avenue, Building 935, Fortaleza, Brazil 60455-760

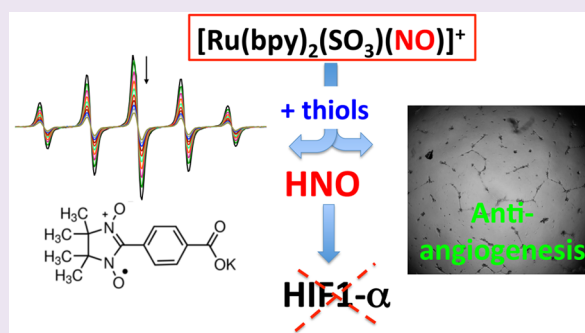
[‡]Department of Chemistry, Federal Institute of Bahia, Salvador, 40301-150, Brazil

[§]Department of Chemistry, University of Warwick, Coventry CV4 7AL, United Kingdom

^{||}National Cancer Institute, Cancer and Inflammation Program, Frederick, Maryland 21702, United States

S Supporting Information

ABSTRACT: Metallonitrosyl complexes are promising as nitric oxide (NO) donors for the treatment of cardiovascular, endothelial, and pathogenic diseases, as well as cancer. Recently, the reduced form of NO⁻ (protonated as HNO, nitroxyl, azanone, isoelectronic with O₂) has also emerged as a candidate for therapeutic applications including treatment of acute heart failure and alcoholism. Here, we show that HNO is a product of the reaction of the Ru^{II} complex [Ru(bpy)₂(SO₃)(NO)]⁺ (1) with glutathione or *N*-acetyl-*L*-cysteine, using met-myoglobin and carboxy-PTIO (2-(4-carboxyphenyl)-4,4,5,5-tetramethylimidazole-1-oxyl-3-oxide) as trapping agents. Characteristic absorption spectroscopic profiles for HNO reactions with met-myoglobin were obtained, as well as EPR evidence from carboxy-PTIO experiments. Importantly, the product HNO counteracted NO-induced as well as hypoxia-induced stabilization of the tumor-suppressor HIF-1 α in cancer cells. The functional disruption of neovascularization by HNO produced by this metallonitrosyl complex was demonstrated in an *in vitro* angiogenesis model. This behavior is consistent with HNO biochemistry and contrasts with NO-mediated stabilization of HIF-1 α . Together, these results demonstrate for the first time thiol-dependent production of HNO by a ruthenium complex and subsequent destabilization of HIF-1 α . This work suggests that the complex warrants further investigation as a promising antiangiogenesis agent for the treatment of cancer.



Nitric oxide (NO) has emerged as a key biological signaling molecule, and a myriad of physiological and pathophysiological functions have now been revealed which strongly support the medical potential for targeting NOS-derived NO in many disease settings.^{1–5} More recently, the reduced form of NO, called nitroxyl (HNO), has attracted attention for its distinct biological activities.⁶ Toward this end, HNO has promising activity in the cardiovascular system, cancer therapy, and neuronal function.⁶ Importantly, HNO exhibits many activities which are distinct from NO, including its ability to limit the accumulation of the tumor suppressor hypoxia-inducible factor-1 (HIF-1 α). Unfortunately, there are few well-characterized HNO donors available, in contrast to the wide variety of NO donors.⁷ The available HNO donors are mainly organic compounds. Metal-based HNO donors are scarce even though many examples of metal complexes as NO donors are known.

HNO is highly reactive toward thiols, while NO depends directly on oxygen-mediated processes that cause thiol modification.⁶ Moreover, HNO exhibits a distinct pattern of thiol modifications when compared to NO, including the

conversion of thiols to sulfinamides, disulfides, and sulfenic acids, instead of thiol nitrosation.^{6,8,9} Protein thiol modification has been associated with some biological activities ascribed to HNO. Two well-described enzymatic systems, glyceraldehyde-3-phosphate dehydrogenase (GADPH)^{8,10} and aldehyde dehydrogenase, are direct targets for HNO, and other suggested targets include cathepsin B and papain.¹¹ These enzymes share similar reactivity profiles: they are inhibited by reaction of HNO with their functional thiols. Another target of HNO is hypoxia-regulated transcription factor HIF-1 α . Importantly, HNO and NO show divergent regulatory effects on HIF-1 α as HNO limits hypoxia- and NO-mediated HIF-1 α protein stabilization. This observation makes HNO an attractive candidate for cancer therapy because NO and HIF-1 α mediate several signaling cascades involved in the disease progression of cancer.^{12–15}

Received: March 9, 2016

Accepted: May 18, 2016

Published: May 18, 2016

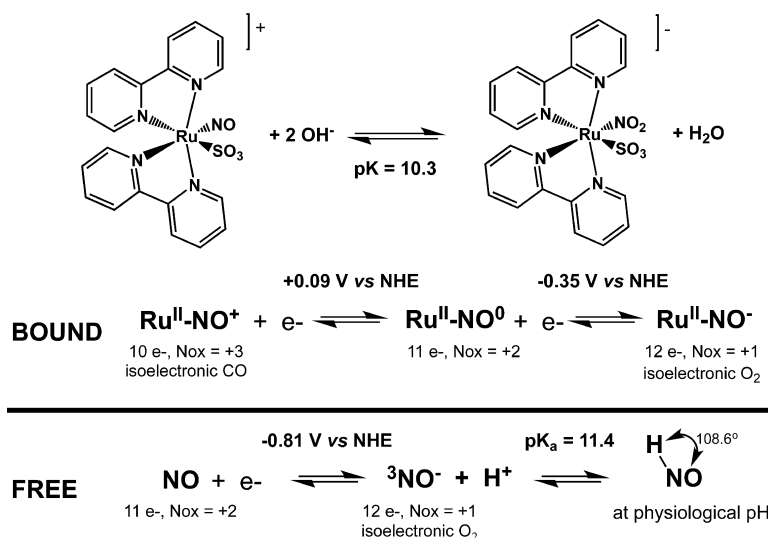


Figure 1. Complex $[\text{Ru}(\text{bpy})_2(\text{SO}_3)(\text{NO})]^+$ (**1**) in an acid–base equilibrium, along with the electrochemical processes associated with the bound nitrosyl moiety and free NO in solution.

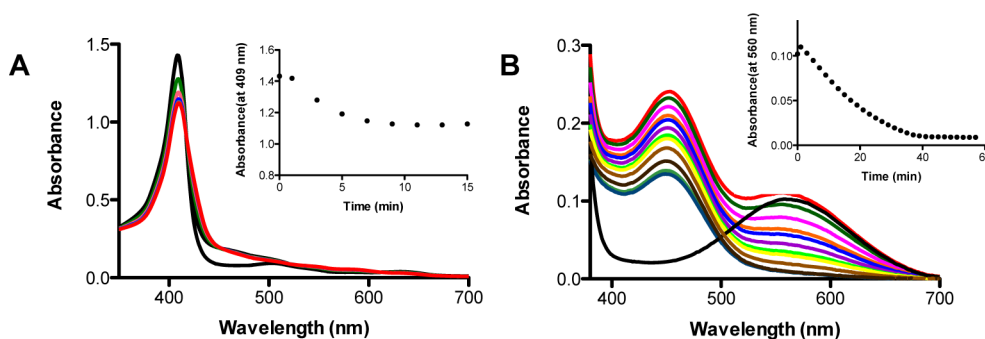


Figure 2. Detection of HNO during reaction of $[\text{Ru}(\text{bpy})_2(\text{SO}_3)(\text{NO})]^+$ with thiols in 0.1 M phosphate buffer at a pH of 6.3, using (A) myoglobin (7.8 μM) and $[\text{Ru}(\text{bpy})_2(\text{SO}_3)(\text{NO})]^+$ (15 μM) with reduced glutathione (200 μM), time-course spectra (inset: reaction kinetics monitored at 409 nm); (B) carboxy-PTIO (100 μM), $[\text{Ru}(\text{bpy})_2(\text{SO}_3)(\text{NO})]^+$ (50 μM), and N-acetylcysteine (200 μM), time-course spectra, black-line spectra before addition of glutathione (inset: reaction kinetics monitored at 560 nm).

The use of ruthenium complexes in medicine has greatly expanded, with some compounds advancing in human clinical trials after demonstrating very low toxicity.^{16–18} These important findings have motivated the scientific community and have led to the development of a wide number of metal-based compounds.¹⁶ Particularly, nitrosyl ruthenium complexes (e.g., $\text{Ru}^{\text{II}}\text{-NO}^+$) have been developed and investigated as NO donors by many laboratories including ours.^{19–22} Interestingly, these metal complexes release NO upon chemical reduction or by light irradiation.^{23,24} One key strategy for NO release that has physiological potential relies on the modulation of the NO^+/NO^0 reduction process where reduction drives the dissociation of NO. This reaction can be altered by the type of ancillary ligand (σ -donor, π -acceptor), which controls the electrochemical potential for bound NO as well as its bonding strength.¹⁹ Bioreductants also show promising ability to generate NO.^{23,25} We have developed a series of nitrosyl complexes based on ruthenium bipyridine chemistry that show promising biological activity including vasodilation activity,²⁶ neuroprotection during ischemia/reperfusion in the brain,²⁷ anti-Chagas disease,²⁸ antiparasitocidal activity,²⁹ gastric protection,³⁰ and analgesic effects.³¹ Among these is the sulfite complex $[\text{Ru}(\text{bpy})_2(\text{SO}_3)(\text{NO})]^+$ (**1**; Figure 1). Interestingly, the presence of the sulfite ligand differentiates **1**

from most nitrosyl ruthenium complexes of this type as it modulates the acid–base equilibrium for bound $\text{NO}^+/\text{NO}_2^-$, which is only shifted toward NO_2^- at higher pH ($pK_a = 10.32$).²⁵ This property can maximize the presence of bound NO^+ at physiological pH, which might have implications for its reactivity toward nucleophiles, particularly thiols. Also, the electrochemical reduction potential $E_{1/2}$ of -115 mV versus Ag/AgCl is within a range accessible for biological reduction. While the reaction with biological thiols has previously provided qualitative evidence for NO production,²³ a detailed quantitative study has yet to be reported, including attempts to detect other NO derivative species, e.g., HNO. Here, we present evidence for the production of HNO triggered by the reaction of $[\text{Ru}(\text{bpy})_2(\text{SO}_3)(\text{NO})]^+$ (**1**) complex with biological thiols and its involvement in key biological activities involving HIF-1 α .

RESULTS

The nitrosyl ruthenium complex stability was investigated by monitoring changes in the electronic spectrum and the electrochemical process at -115 mV (vs Ag/AgCl). No significant changes were observed in the UV–vis electronic spectra of a 40 μM solution of $[\text{Ru}(\text{bpy})_2(\text{SO}_3)(\text{NO})]^+$ in 5 mM phosphate buffer at a pH of 7.4 and 100 mM NaCl at 37

°C during 12 h of incubation (Supporting Information Figure S1A). Similarly, differential pulse voltammetry did not show significant electrochemical changes at -115 mV, which is assigned to $\text{Ru}^{\text{II}}\text{-NO}^{+/0}$ during 10 h of incubation (Supporting Information Figure S1B).

Biothiol-Induced Production of Nitroxyl Species. A well-described assay for HNO detection employs ferric-myoglobin (met-Mb), which also distinguishes HNO from NO.^{32–34} In this assay, HNO reduces met(Fe^{III})-myoglobin, giving ferrous(Fe^{II})-NO myoglobin, and a typical red shift of the Soret band as well as changes to the Q-bands are observed. Here, we used a slight molar excess of metallonitrosyl complex **1** to met-myoglobin to evaluate HNO production upon reaction with glutathione (GSH, γ -L-Glu-L-Cys-Gly) or N-acetyl-L-cysteine (NAC), a precursor of glutathione. We should further mention that NO can eventually react with met(Fe^{III})-myoglobin, but the rate is slow and affinity ($K_{\text{d}} \sim 260 \mu\text{M}$) very weak, requiring much larger amounts of NO than ferrous(Fe^{II})-myoglobin.^{35,36} Additionally, $\text{Fe}^{\text{III}}\text{-NO}$ myoglobin shows distinct spectroscopic features (Soret and Q-band maxima) as compared to $\text{Fe}^{\text{II}}\text{-NO}$ myoglobin, a result of a fast HNO reaction.³⁵ A series of controls were prepared to evaluate the occurrence of any direct reaction between ferric-myoglobin and the metallonitrosyl compound or thiols (glutathione and N-acetyl-L-cysteine) alone, as well as using a standard HNO donor (Angeli's salt) and NO donor (DEA-NONOATE; Supporting Information Figure S2). When this reaction was carried out with $[\text{Ru}(\text{bpy})_2(\text{SO}_3)(\text{NO})]^+$ and the thiol together with met-Mb, a typical change in the ferric myoglobin UV-vis spectra was observed consistent with HNO production (Figure 2). After longer incubation times, reoxidation of myoglobin was also observed for control reactions using only the HNO donor (Angeli's salt) as reported elsewhere.³³

The HNO probe carboxy-PTIO (cPTIO) was used to further validate these results. Carboxy-PTIO (cPTIO) is a stable radical well-known as a stoichiometric NO scavenger and suitable EPR probe for the *in vitro* detection of NO.³⁷ However, this probe has notable limitations for *in vivo* detection of NO due to side reactions with other biological reducing species.³⁸ Recently, detailed studies have shown that cPTIO can be used to distinguish NO from HNO, based on differences in the resulting EPR signals.³⁹ cPTIO reacts with stoichiometric amounts of NO, yielding an increased number of EPR lines from 5 ($a_{\text{N}}^{1,3} = 8.1$ G) to 7 due to the appearance of a nonsymmetrical nitrogen leading to different hyperfine splitting constants for ^{14}N ($a_{\text{N}}^1 = 9.8$ G and $a_{\text{N}}^3 = 4.4$ G).³⁷ On the other hand, HNO has been reported to react rapidly with stoichiometric amounts of cPTIO leading to an EPR-silent product (PTI).⁴⁰ Electronic spectral changes are also observed for cPTIO in reaction with HNO and NO, where a band at 560 nm equally disappears, while other changes at lower wavelengths can be used to distinguish them.⁴⁰ Unfortunately, those bands could not be used unequivocally in our studies due to interference in the same range from the metal complex itself. So, we used the band at 560 nm to assign NO or HNO production (Figure 2), whereas the EPR signal was used to differentiate between them (Figure 3). Similar to the reactions with met-Mb, a series of controls were used to validate the EPR signals and eliminate possible interferences (Supporting Information Figures S3 and S4).

Reactions of $[\text{Ru}(\text{bpy})_2(\text{SO}_3)(\text{NO})]^+$ with GSH or NAC gave rise to the rapid disappearance of the 560 nm band of cPTIO, suggesting that NO or HNO was indeed generated

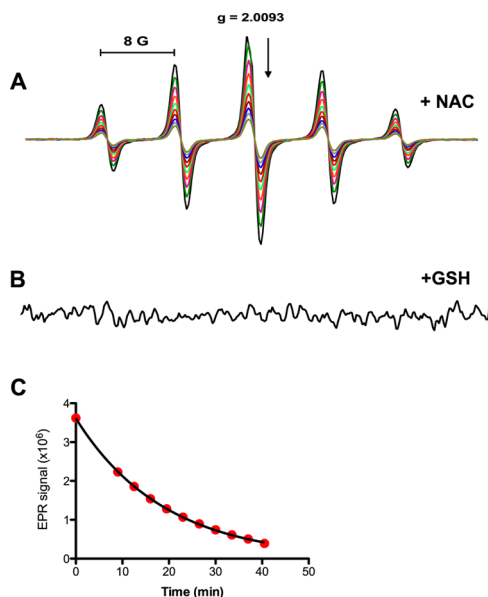
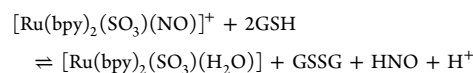
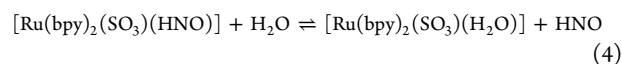
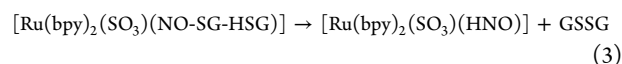
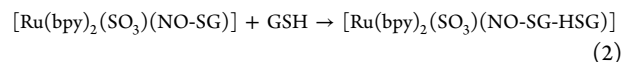
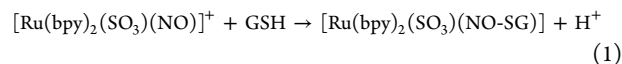


Figure 3. EPR detection of HNO using the radical carboxy-PTIO ($200 \mu\text{M}$) in 0.1 M phosphate buffer at a pH of 6.3, from reactions of $[\text{Ru}(\text{bpy})_2(\text{SO}_3)(\text{NO})]^+$ ($50 \mu\text{M}$) with (A) N-acetyl-L-cysteine ($800 \mu\text{M}$) and (B) glutathione ($800 \mu\text{M}$). (C) kinetic profile for EPR signal from experiment A.

during these reactions (Figure 2). EPR spectra showed the disappearance of the EPR signal, supporting HNO production (Figure 3). This metal complex has been shown to photorelease NO,²⁵ and we verified this by EPR, observing peaks typical of NO trapping by cPTIO (Supporting Information Figure S4). These EPR data therefore confirmed that $[\text{Ru}(\text{bpy})_2(\text{SO}_3)(\text{NO})]^+$ mainly generates HNO on reaction with thiols, while light promotes NO release. Also, we showed that reaction with excess GSH can produce hydroxylamine, a well-described final product for the reaction of HNO with excess glutathione.⁴¹ Hydroxylamine was detected from reactions of both Angeli's salt and $[\text{Ru}(\text{bpy})_2(\text{SO}_3)(\text{NO})]^+$ (Supporting Information Figure S5).

^1H NMR spectra were also recorded for the reaction of $[\text{Ru}(\text{bpy})_2(\text{SO}_3)(\text{NO})]^+$ with GSH at 1:0.5, 1:1, and 1:2 molar ratios of the Ru complex to GSH. At a ratio of 1:2, the spectra were consistent with complete production of oxidized glutathione, which is expected for a reaction involving two-electron transfer from thiols to generate nitroxyl from the original nitronium reagent (Figure 1, Supporting Information Figure S6) as described by the possible sequence of reactions 1–4.



Electrochemical studies were also conducted for the reaction of $[\text{Ru}(\text{bpy})_2(\text{SO}_3)(\text{NO})]^+$ with GSH using square-wave voltammetry in 0.1 M phosphate buffer at a pH of 7.4 using Ag/AgCl as a reference. $[\text{Ru}(\text{bpy})_2(\text{SO}_3)(\text{NO})]^+$ showed two sets of signals, one at -115 mV assigned to $\text{NO}^{+/0}$ processes and another two peaks at -640 to -510 mV. The latter can be assigned to reduction of NO^0 to NO^- at -510 mV and a further reduction of NO^- to NH_3 at -640 mV, as reported for other similar systems.⁴² These signals were greatly perturbed by the addition of reduced glutathione (Figure 4). Almost

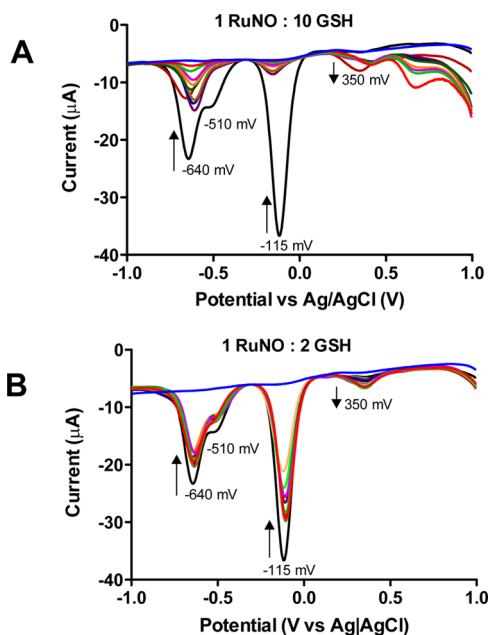


Figure 4. Electrochemical response of $[\text{Ru}(\text{bpy})_2(\text{SO}_3)(\text{NO})]^+$ (1 mM) in reactions with glutathione in 0.1 M phosphate buffer at a pH of 7.4, followed by square-wave voltammetry (glassy carbon as the working electrode and Ag/AgCl as the reference electrode, reductive sweep). (A) 10-fold molar excess of reduced glutathione (10 mM); (B) 2-fold excess of glutathione (2 mM), monitored for 30 min.

immediately after the addition of a 15-fold molar excess of glutathione, the waves at -115 mV and -510 mV disappeared, which is consistent with reaction of the NO^+ ligand to give NO^- , followed by a new wave at -580 mV with a slower change. New waves at $+350$ mV and $+665$ mV can also be assigned to $\text{Ru}^{\text{III/II}}$ processes for $[\text{Ru}(\text{bpy})_2(\text{SO}_3)(\text{H}_2\text{O})]$ and $[\text{Ru}(\text{bpy})_2(\text{SO}_3)(\text{NH}_3)]$, respectively. Measurements conducted with close to stoichiometric amounts of GSH (1 to 10-fold) supported fast disappearance of $\text{NO}^{+/0}$ processes due to prompt reduction of this species, along with consumption of the signal assigned to $\text{NO}^{0/-}$ seen as a shoulder at -510 mV. The main peak at very low reduction potential has been assigned to the conversion of NO^- to NH_3 .⁴² Interestingly, this signal was slightly affected, consistent with generation of Ru-NO^- . Moreover, depending on the amount of excess glutathione, it was possible to reach complete consumption of NO^- , which suggests an equilibrium shift may be involved. Since an excess of glutathione can react rapidly with free HNO, it is possible to shift the equilibrium for Ru-HNO to favor the release of HNO, as indicated by eq 4.

HIF-1 α Stabilization Induced by NO or Hypoxia. Hypoxia-inducible factor-1 (HIF-1) is a transcription factor composed of HIF-1 α and HIF-1 β subunits, which regulates

cellular response to oxygen. While HIF-1 β is constitutively expressed, HIF-1 α protein levels are minimal or undetectable under normoxic conditions. During hypoxia, HIF-1 α protein is stabilized and translocated to the nucleus where its dimerization with HIF-1 β leads to HIF-1 binding at hypoxia responsive elements (HRE) in many target genes including those involved in angiogenesis and cellular metabolism. In cancer, HIF-1 α dysregulation and/or overexpression promotes tumor growth and metastasis by regulating tumor angiogenesis, cellular metabolism, and survival in response to tumor hypoxia, thus making HIF-1 α an attractive chemotherapeutic target.⁴³ It is widely understood that normoxia regulates the protein stability and turnover of HIF-1 α , through hydroxylation of two key proline residues (Pro402 and Pro564) by prolyl hydroxylase (PHD), which targets HIF-1 α for ubiquitination and proteasomal degradation.^{44,45} Interestingly, S-nitrosation by NO attenuates PHD activity and stabilizes HIF-1 α protein levels under normoxic conditions.^{13,46,47} With this in mind, we examined the effect of $[\text{Ru}(\text{bpy})_2(\text{SO}_3)(\text{NO})]^+$ complex on NO- or hypoxia-induced HIF-1 α protein stabilization in MB-231 and MCF-7 breast cancer cells. Thomas *et al.* have shown HIF-1 α stabilization following exposure to the NO donor SPER/NO (4 h).¹³ Pretreatment (30 min) of MB-231 breast cancer cells with $10 \mu\text{M}$ $[\text{Ru}(\text{bpy})_2(\text{SO}_3)(\text{NO})]^+$ (1) abated SPER/NO-induced HIF-1 α stabilization as shown in Figure 5A,B. The control compound $[\text{Ru}(\text{bpy})_2(\text{SO}_3)(\text{H}_2\text{O})]^+$ (2) did not alter significantly the level of SPER/NO induced HIF-1 α (only $\sim 25\%$). Abated HIF-1 α levels by HNO released from the $[\text{Ru}(\text{bpy})_2(\text{SO}_3)(\text{NO})]^+$ complex are consistent with the observations of Norris *et al.*, who demonstrated that HNO produced by Angeli's salt also attenuated HIF-1 α protein levels in MB-231 and MCF-7 cells when compared to controls.¹² Importantly, $10 \mu\text{M}$ $[\text{Ru}(\text{bpy})_2(\text{SO}_3)(\text{NO})]^+$ alone did not induce HIF-1 α stabilization (Figure 5A,B), indicating that under these conditions $[\text{Ru}(\text{bpy})_2(\text{SO}_3)(\text{NO})]^+$ released HNO but not NO. Interestingly, Figure 5C shows that SPER/NO-induced HIF-1 α stabilization was not effected by YC-1 (3-(5'-hydroxymethyl-2'-furyl)-1-benzyl indazole), a known Akt-dependent inhibitor of hypoxia-induced HIF-1 α .⁴⁸ $[\text{Ru}(\text{bpy})_2(\text{SO}_3)(\text{NO})]^+$ also significantly disrupted hypoxia-induced HIF-1 α (Figure 5D,E); however it was less efficient when compared to YC-1. Importantly, a functional *in vitro* angiogenesis assay demonstrated a dramatic reduction in endothelial tube formation by $[\text{Ru}(\text{bpy})_2(\text{SO}_3)(\text{NO})]^+$ as shown in Figure 5F,G. Together these results provide evidence of anti-HIF and antiangiogenic effects by thiol-dependent release of HNO from $[\text{Ru}(\text{bpy})_2(\text{SO}_3)(\text{NO})]^+$ applied in biological systems.

DISCUSSION

Here, we have employed two different probes, ferric-myoglobin and carboxy-PTIO, to investigate production of HNO from reactions of $[\text{Ru}(\text{bpy})_2(\text{SO}_3)(\text{NO})]^+$ (1) with thiols. These reactions generated a species compatible with HNO as indicated by the two detection methods (Figures 2 and 3). Ferric myoglobin exhibited a typical lowering and red shift of the Soret band along with the appearance of two bands in the Q-band region, indicative of ferrous-NO myoglobin generation. This behavior mirrored a control reaction using a known HNO donor. Moreover, $[\text{Ru}(\text{bpy})_2(\text{SO}_3)(\text{NO})]^+$ did not react with ferric-myoglobin at all, even upon light irradiation, unless thiols were added. In addition, cPTIO provided additional evidence of HNO production triggered by thiols as supported by the

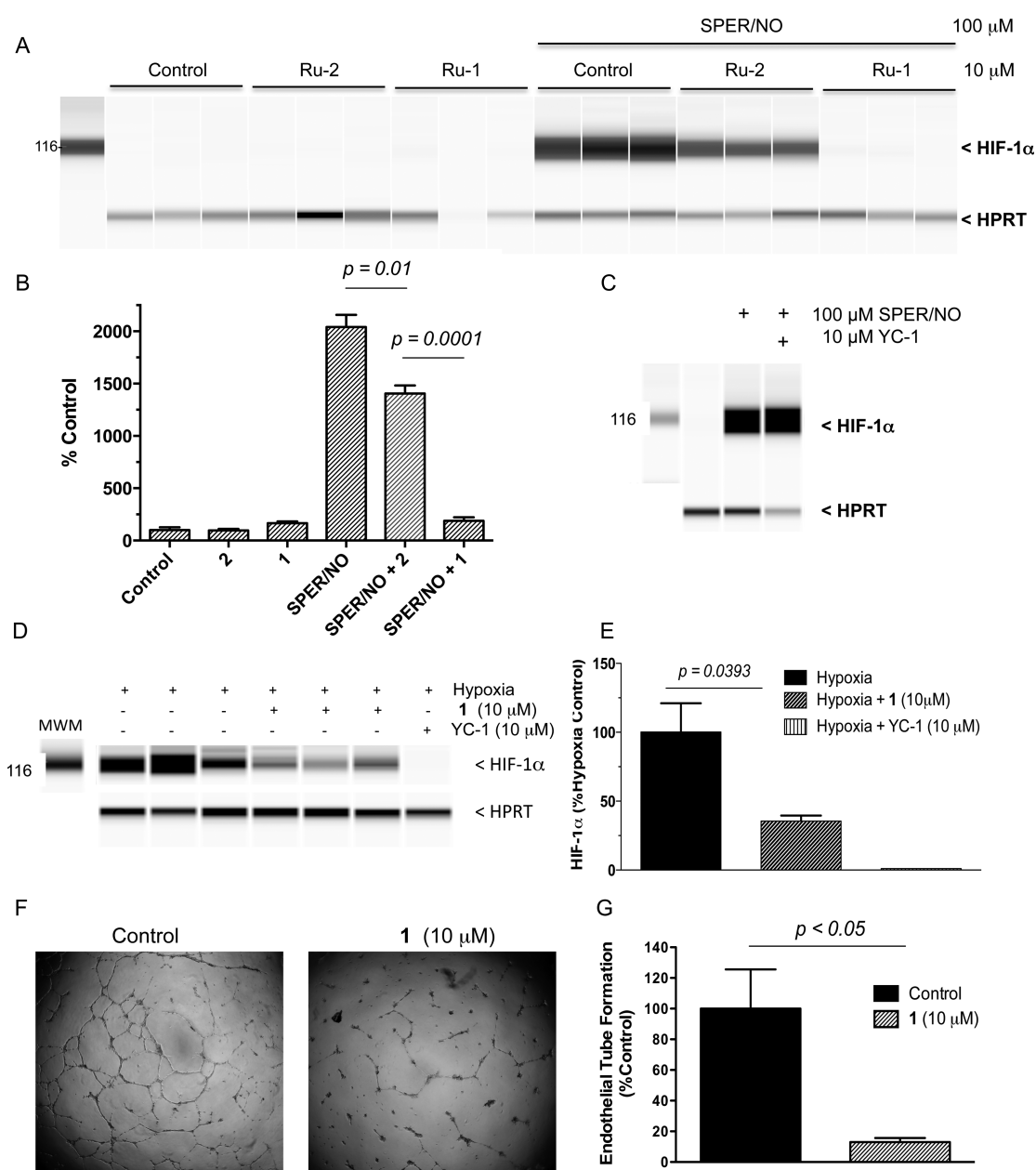


Figure 5. Limitation of HIF-1 α stabilization by [Ru(bpy)₂(SO₃)(NO)]⁺ (**1**) in breast cancer cells treated with 100 μ M SPER/NO or under hypoxia. (A) Western blot of HIF-1 α and HPRT housekeeping control protein levels in MB-231 breast cancer cells pretreated with 10 μ M **1** or [Ru(bpy)₂(SO₃)(H₂O)] control (**2**) for 30 min prior to HIF-1 α stimulation (4 h) by the NO donor SPER/NO (100 μ M). (B) Quantitative measurement of HIF-1 α normalized to HPRT in MB-231 cell lysates shown in A. (C) YC-1, a known inhibitor of hypoxia-induced HIF-1 α fails to block HIF-1 α stabilization by SPER/NO. (D) Western blot of HIF-1 α and HPRT housekeeping control in MCF-7 breast cancer cells flushed with N₂ gas for 1.5 h to create hypoxic conditions. YC-1 is included as a positive control, which inhibits hypoxia induced HIF-1 α protein accumulation. (E) A quantitative measurement of HIF-1 α normalized to HPRT shown in panel D. (F) Abated HUVEC tube formation in *in vitro* angiogenesis assay along with (G) quantitative measurements of enclosed and partially enclosed networks in [Ru(bpy)₂(SO₃)(NO)]⁺-treated cells versus control.

disappearance of its EPR signal. Interestingly, there was no evidence of NO release using cPTIO as a probe, which did not show an increase in the number of EPR lines. Indeed, such behavior was observed only upon light irradiation of [Ru(bpy)₂(SO₃)(NO)]⁺ (Supporting Information Figure S4), which is known to photorelease NO.²⁵ Our earlier quantitative work suggested that NO is released upon reactions with thiols.²³ While minimal NO can still be produced, the present work shows that HNO is clearly the main species generated and the most likely product of thiol activation of such metal-nitrosyl complexes. Other investigators have also suggested

that reactions of metallonitrosyl complexes with thiols can lead to alternative routes producing either NO or HNO.⁴⁹

NMR results supported the production of oxidized glutathione from reactions in a stoichiometry of 2:1 GSH/Ru(bpy)₂(SO₃)(NO)]⁺, consistent with a two-electron process yielding NO⁻. Electrochemical data also showed evidence for suppression of the reduction process assigned to NO⁺⁰ as well as for NO^{0/-}, upon the addition of glutathione. Previous kinetic studies showed spectroscopic evidence of an adduct,²³ which might release oxidized glutathione and give rise to Ru-HNO. It is reasonable to assume modest release of HNO. Indeed, there

are examples of reasonably stable metal complexes containing HNO, such as $[\text{Fe}(\text{CN})_5(\text{HNO})]^{3-}$ where the extent of HNO release is modest and quite slow ($k_{\text{off}} < 4.7 \times 10^{-7} \text{ s}^{-1}$).⁵⁰ $[\text{Ru}(\text{bpy})_2(\text{SO}_3)(\text{H}_2\text{O})]$ is assigned as one final product from the present reaction with thiols and shows intense band at 450 nm.²³

Studies of a series of ruthenium nitrosyl complexes have shown that $[\text{Ru}(\text{bpy})_2(\text{SO}_3)(\text{NO})]^+$ exhibits promising trypanocidal activity against *Trypanosoma cruzi* by promoting higher survival rates in infected mice.²⁸ Additionally, this metal complex inhibits *T. cruzi* GAPDH enzymatic activity, which is thought to be its physiological target. The crystal structure of GAPDH following the reaction with $[\text{Ru}(\text{bpy})_2(\text{SO}_3)(\text{NO})]^+$ suggested an NO-mediated thiol modification.²⁸ However, the specific thiol modification did not resemble S-nitrosylation, as would be expected for an NO mechanism. In contrast, the modification was consistent with sulfinamide or sulfinic acid adducts caused by HNO. Interestingly, one of the best-described biological targets of HNO is indeed GAPDH, where the thiol modification generated a sulfinamide or sulfinic acid moiety.⁸

Additionally, HIF-1 α degradation promoted by HNO was earlier thought to be associated with the direct effect of HNO on GAPDH activity.¹² This phenomenon is associated with a fast reaction of HNO with a GAPDH active cysteine residue generating a sulfonamide modification that culminated in the disruption of glycolytic pathways.¹² On the basis of this evidence, it is reasonable to suggest the reduction of HIF-1 α protein could result from GAPDH inhibition promoted by this metal complex.

Herein, the chemical evidence for HNO generation from $[\text{Ru}(\text{bpy})_2(\text{SO}_3)(\text{NO})]^+$ was validated biologically by the demonstration of reduced HIF-1 α protein accumulation in cancer cells treated with NO or hypoxia. Similar effects of HNO produced by Angeli's salt on abated HIF-1 α accumulation in cancer cells was shown earlier and is fully consistent with our studies using a metallonitrosyl complex.¹² As far as we are aware, these results provide the first biological evidence of anticancer effects of a metal complex acting as an HNO donor. Vascularization is a very important process in physiological and pathological conditions; its inhibition can be therapeutically beneficial in the treatment of cancer.⁵² Solid tumors grow at a very fast rate and require increased neo-vascularization to support the necessary supply of oxygen and nutrient requirements as well as metastatic processes. Blockade of this route provides an opportunity to contain tumor growth and metastatic disease. HIF-1 α is a transcription factor essential for regulating vascularization and VEGF expression, and it is closely regulated by an oxygen-dependent prolyl hydroxylase. Under normoxic conditions, prolyl hydroxylases modify HIF-1 α leading to proteasomal degradation, and low levels of HIF-1 α are maintained. On the other hand, in hypoxic tissue, this post-transcriptional modification is blocked, causing HIF-1 α accumulation, which then upregulates neo-vascularization processes. Only a limited number of compounds that target HIF are under development. Also, HNO and NO exhibit divergent HIF-1 α regulation; NO promotes HIF-1 α stabilization while HNO limits its accumulation. We exploited this divergent behavior as a biological assay to investigate NO versus HNO activity. Our results support the use of $[\text{Ru}(\text{bpy})_2(\text{SO}_3)(\text{NO})]^+$ as a promising therapeutic agent for abated HIF-1 α accumulation. Under hypoxic conditions, $[\text{Ru}(\text{bpy})_2(\text{SO}_3)(\text{NO})]^+$ reduced HIF-1 α however less effec-

tively when compared to YC-1. Moreover, $[\text{Ru}(\text{bpy})_2(\text{SO}_3)(\text{NO})]^+$ dramatically reduced HIF-1 α under conditions of elevated NO. This is significant because YC-1, a leading compound used for the development of new antiangiogenic agents, failed to reduce HIF stabilization induced by NO. Importantly, elevated NOS2-derived NO predicts poor survival in patients with aggressive tumors including estrogen receptor negative breast cancer where NOS2 directly correlated with the vascular marker CD31.⁵³ In addition, high NOS2 expressing tumors exhibited greater than 3-fold elevations in glutamate cysteine ligase, which is the rate-limiting enzyme in the glutathione synthesis pathway, which suggests that patients with this NOS2 signature may benefit from $[\text{Ru}(\text{bpy})_2(\text{SO}_3)(\text{NO})]^+$ or similar drugs.⁵³

Conclusions. The elucidation of HNO biochemistry has led to new discoveries with therapeutic potential, which warrants the development of novel HNO donors. The current study provides evidence that HNO is indeed generated by $[\text{Ru}(\text{bpy})_2(\text{SO}_3)(\text{NO})]^+$ upon reaction with thiols; such reactions could be responsible for several of the biological activities described for this compound so far. Moreover, this and other structurally related compounds are novel HNO donors that are candidate antiangiogenic agents with potential applications in cardiovascular and cancer therapy. The current study demonstrates that the reactivity of bound NO is essential for HNO generation, which warrants further investigation as a new generation of ruthenium nitrosyl complexes, with larger and moderate NO⁺ character for improved thiol-reactive HNO donors.

Potential applications for these ruthenium compounds include anticancer therapy for aggressive breast tumors expressing elevated NOS2 and increased glutamate cysteine ligase, which would enhance tumor glutathione levels. In such tumors, this compound might be quite suitable for therapy and work also as a tool to modulate the levels of thiol-reactive species. Multidrug resistance pathways utilize glutathione to pump drugs out of the cell; HNO-based drugs may be beneficial in the treatment of these resistant tumor phenotypes as well. HNO also affects cellular glucose transport by modulating GLUT1 activity as demonstrated using Angeli's salt.⁵¹ Collectively, these observations have stimulated interest in new therapeutic opportunities for HNO donors, suggesting that this molecule will attract increasing attention in years to come.

METHODS

Materials. N-[4-[1-(3-Aminopropyl)-2-hydroxy-2-nitrosohydrazino]butyl]-1,3-propanediamine (SPER/NO), diethylamine NONOate diethylammonium salt (DEA-NO), sodium trioxodinitrate (Angeli's salt), 2-(4-carboxyphenyl)-4,4,5,5-tetramethylimidazole-1-oxyl-3-oxide potassium salt (carboxy-PTIO, cPTIO), ferric myoglobin (metMb, equine skeletal muscle), reduced glutathione (GSH), oxidized glutathione (GSSG), ascorbic acid, N-acetylcysteine (NAC), trifluoroacetic acid (HTFA), sodium sulphite, bipyridine, ruthenium trichloride, sodium hydroxide, sodium nitrite, $\text{Na}_2\text{H}_2\text{edta}$, Na_2HPO_4 , and NaH_2PO_4 were purchased from Sigma-Aldrich. Organic solvents were all of chromatographic grade. Water used in the experiments and synthesis was ultrapurified using a Milli-Q system (>18 M Ω cm). $[\text{Ru}(\text{bpy})_2(\text{SO}_3)(\text{NO})](\text{PF}_6)$ (1) was prepared as described in the literature and $[\text{Ru}(\text{bpy})_2(\text{SO}_3)(\text{H}_2\text{O})]$ (2) as in ref 25.

Myoglobin As a Probe for HNO Production. To detect HNO production, ferric-myoglobin at a 7–8 μM final concentration in 0.1 M phosphate buffer at a pH of 6.3 at 25 °C was employed. See the Supporting Information for details.

Carboxy-PTIO Reaction to Identify HNO. Carboxy-PTIO was used to probe HNO and NO formation as characterized by characteristic changes in their UV–vis and EPR spectra. This organic spin-trap was used at 100–200 μM in 0.1 M phosphate buffer at a pH of 6.3 along with reduced glutathione and N-acetyl-cysteine alone and in reaction with $[\text{Ru}(\text{bpy})_2(\text{SO}_3)(\text{NO})]^+$ as well as upon light irradiation. See the [Supporting Information](#) for details.

Hydroxylamine Detection. This measurement was conducted as described elsewhere⁵⁴ with minor modifications.⁵⁵ See the [Supporting Information](#) for details.

NMR Studies of Reactions of Ru Complex with Glutathione. ^1H NMR spectra were recorded on a Bruker AV111–400 spectrometer for 7.2 mM solutions of $[\text{Ru}(\text{bpy})_2(\text{SO}_3)(\text{NO})]^+$ with 1 mol equiv of sodium azide, or 0.5, 1.0, or 2.0 mol equiv of glutathione in phosphate buffer/ D_2O at a pH of 7.4 at 298 K.

Electrochemistry Measurements. Square-wave voltammetry was used to measure the half-wave potential of 0.8 mM $[\text{Ru}(\text{bpy})_2(\text{SO}_3)(\text{NO})]^+$, before and after the addition of reduced glutathione (1 mM to 15 mM), in argon degassed 0.1 M phosphate buffer (pH 7.4) as an electrolyte, at 298 K. These measurements were performed in an electrochemical analyzer from Bioanalytical System Inc. (BAS) model EPSILON, using a conventional electrochemical glass cell containing three electrodes: glassy carbon as a working electrode, Ag|AgCl as a reference electrode, and platinum foil as an auxiliary electrode.

HIF-1 α Inhibition Assay. MCF-7 or MB-231 breast cancer cells (2×10^6 cells) were plated into 60 mm cell culture dishes in RPMI complete medium supplemented with 10% HI FBS and penicillin-streptomycin and incubated overnight. The next day, the cells were pretreated with the metallonitrosyl **1** $[\text{Ru}(\text{bpy})_2(\text{SO}_3)(\text{NO})](\text{PF}_6)$ or control **2** compound ($[\text{Ru}(\text{bpy})_2(\text{SO}_3)(\text{H}_2\text{O})]$) for 30 min in serum-free medium, then treated with 100 μM SPER/NO for 4 h. See the [Supporting Information](#) for details.

Automated Capillary Western Blot (WES). Western blots were performed using WES, an automated capillary-based size sorting system (ProteinSimple, San Jose CA).⁵⁶ All procedures were performed with the manufacturer's reagents according to their user manual. See the [Supporting Information](#) for details.

In Vitro Angiogenesis Assay. Antiangiogenic effects were examined using an *in vitro* angiogenesis assay kit (EMD Millipore, Billerica MA) according to the manufacturer's recommendations. See the [Supporting Information](#) for details.

■ ASSOCIATED CONTENT

■ Supporting Information

The Supporting Information is available free of charge on the ACS Publications website at DOI: [10.1021/acscchembio.6b00222](https://doi.org/10.1021/acscchembio.6b00222).

Experimental Details and Figures S1–S6 ([PDF](#))

■ AUTHOR INFORMATION

Corresponding Authors

*E-mail: eduardohss@dqoi.ufc.br.

*E-mail: p.j.sadler@warwick.ac.uk.

Author Contributions

E.H.S.S., L.A.R., D.A.W., L.G.d.F.L., and P.J.S. designed the experiments. E.H.S.S., L.A.R., F.S.G. Jr., and C.D.S.d.S. carried out the experiments. E.H.S.S., L.A.R., F.S.G. Jr., D.A.W., L.G.d.F.L., and P.J.S. analyzed and interpreted data. E.H.S.S., L.A.R., D.A.W., L.G.d.F.L., and P.J.S. wrote the manuscript

Notes

The authors declare no competing financial interest.

■ ACKNOWLEDGMENTS

The authors are thankful to Brazilian agencies CAPES, CNPq (L.G.d.F.L. 303732/2014-8, E.H.S.S. 312030/2015-0), FUNCAP (PPSUS 12535691-9), the European Research Council

(grant no 247450 to P.J.S.), and Engineering and Physical Sciences Research Council (grant no. EP/F034210/1 to P.J.S.) and the Intramural Research Program of the NIH, Cancer and Inflammation Program (LAR) for financial support.

■ REFERENCES

- (1) Lincoln, T. M., and Komalavilas, P. (2000) *Nitric Oxide: Biology and Pathobiology*, Academic Press, San Diego.
- (2) Wink, D. A., Ridnour, L. A., Hussain, S. P., and Harris, C. C. (2008) The reemergence of nitric oxide in cancer. *Nitric Oxide* 19, 65–67.
- (3) Lo Faro, M. L., Fox, B., Whatmore, J. L., Winyard, P. G., and Whiteman, M. (2014) Hydrogen sulfide and nitric oxide interactions in inflammation. *Nitric Oxide* 41, 38–47.
- (4) Thomas, D. D., Ridnour, L. A., Isenberg, J. S., Flores-Santana, W., Switzer, C. H., Donzelli, S., Hussain, P., Vecoli, C., Paolucci, N., Ambs, S., Colton, C. A., Harris, C. C., Roberts, D. D., and Wink, D. A. (2008) The chemical biology of nitric oxide: implications in cellular signaling. *Free Radical Biol. Med.* 45, 18–31.
- (5) Hetrick, E. M., Shin, J. H., Paul, H. S., and Schoenfisch, M. H. (2009) Anti-biofilm efficacy of nitric oxide-releasing silica nanoparticles. *Biomaterials* 30, 2782–2789.
- (6) Flores-Santana, W., Salmon, D. J., Donzelli, S., Switzer, C. H., Basudhar, D., Ridnour, L., Cheng, R., Glynn, S. A., Paolucci, N., Fukuto, J. M., Miranda, K. M., and Wink, D. A. (2011) The specificity of nitroxyl chemistry is unique among nitrogen oxides in biological systems. *Antioxid. Redox Signaling* 14, 1659–1674.
- (7) Nakagawa, H. (2013) Controlled release of HNO from chemical donors for biological applications. *J. Inorg. Biochem.* 118, 187–190.
- (8) Mitroka, S., Shoman, M. E., DuMond, J. F., Bellavia, L., Aly, O. M., Abdel-Aziz, M., Kim-Shapiro, D. B., and King, S. B. (2013) Direct and nitroxyl (HNO)-mediated reactions of acyloxy nitroso compounds with the thiol-containing proteins glyceraldehyde 3-phosphate dehydrogenase and alkyl hydroperoxide reductase subunit C. *J. Med. Chem.* 56, 6583–6592.
- (9) Keceli, G., and Toscano, J. P. (2014) Reactivity of C-terminal cysteines with HNO. *Biochemistry* 53, 3689–3698.
- (10) Lopez, B. E., Wink, D. A., and Fukuto, J. M. (2007) The inhibition of glyceraldehyde-3-phosphate dehydrogenase by nitroxyl (HNO). *Arch. Biochem. Biophys.* 465, 430–436.
- (11) DeMaster, E. G., Redfern, B., and Nagasawa, H. T. (1998) Mechanisms of inhibition of aldehyde dehydrogenase by nitroxyl, the active metabolite of the alcohol deterrent agent cyanamide. *Biochem. Pharmacol.* 55, 2007–2015.
- (12) Norris, A. J., Sartippour, M. R., Lu, M., Park, T., Rao, J. Y., Jackson, M. I., Fukuto, J. M., and Brooks, M. N. (2008) Nitroxyl inhibits breast tumor growth and angiogenesis. *Int. J. Cancer* 122, 1905–1910.
- (13) Thomas, D. D., Espey, M. G., Ridnour, L. A., Hofseth, L. J., Mancardi, D., Harris, C. C., and Wink, D. A. (2004) Hypoxic inducible factor 1 α , extracellular signal-regulated kinase, and p53 are regulated by distinct threshold concentrations of nitric oxide. *Proc. Natl. Acad. Sci. U. S. A.* 101, 8894–8899.
- (14) Balamurugan, K. (2016) HIF-1 at the crossroads of hypoxia, inflammation, and cancer. *Int. J. Cancer* 138, 1058–1066.
- (15) Ambs, S., and Glynn, S. A. (2011) Candidate pathways linking inducible nitric oxide synthase to a basal-like transcription pattern and tumor progression in human breast cancer. *Cell Cycle* 10, 619–624.
- (16) Barry, N. P., and Sadler, P. J. (2013) Exploration of the medical periodic table: towards new targets. *Chem. Commun. (Cambridge, U. K.)* 49, 5106–5131.
- (17) Leijen, S., Burgers, S. A., Baas, P., Pluim, D., Tibben, M., van Werkhoven, E., Alessio, E., Sava, G., Beijnen, J. H., and Schellens, J. H. (2015) Phase I/II study with ruthenium compound NAMI-A and gemcitabine in patients with non-small cell lung cancer after first line therapy. *Invest. New Drugs* 33, 201–214.
- (18) Hartinger, C. G., Jakupec, M. A., Zorbas-Seifried, S., Groessl, M., Egger, A., Berger, W., Zorbas, H., Dyson, P. J., and Keppler, B. K.

- (2008) KP1019, a new redox-active anticancer agent—preclinical development and results of a clinical phase I study in tumor patients. *Chem. Biodiversity* 5, 2140–2155.
- (19) Tfouni, E., Doro, F. G., Figueiredo, L. E., Pereira, J. C. M., Metzke, G., and Franco, D. W. (2010) Tailoring NO Donors Metallopharmaceuticals: Ruthenium Nitrosyl Amines and Aliphatic Tetraazamacrocycles. *Curr. Med. Chem.* 17, 3643–3657.
- (20) da Silva, F. O. N., Gomes, E. C. C., Francisco, T. D., Holanda, A. K. M., Diógenes, I. C. N., de Sousa, E. H. S., Lopes, L. G. F., and Longhinotti, E. (2010) NO donors cis-[Ru(bpy)₂(L)NO]³⁺ and [Fe(CN)₄(L)NO][−] complexes immobilized on modified mesoporous silica spheres. *Polyhedron* 29, 3349–3354.
- (21) Lopes, L. G. F., Sousa, E. H. S., Miranda, J. C. V., Oliveira, C. P., Carvalho, I. M. M., Batista, A. A., Ellena, J., Castellano, E. E., Nascimento, O. R., and Moreira, I. S. (2002) Crystal structure, electrochemical and spectroscopic properties of the trans-K₂[FeCl(NO⁰) (cyclam)]·[FeCl(NO⁺) (cyclam)]₂(PF₆)₆ complex. *J. Chem. Soc.-Dalton Trans.*, 1903–1906.
- (22) Tfouni, E., Truzzi, D. R., Tavares, A., Gomes, A. J., Figueiredo, L. E., and Franco, D. W. (2012) Biological activity of ruthenium nitrosyl complexes. *Nitric Oxide* 26, 38–53.
- (23) Silva, F. O. N., Candido, M. C. L., Holanda, A. K. M., Diógenes, I. C. N., Sousa, E. H. S., and Lopes, L. G. F. (2011) Mechanism and Biological Implications of the NO Release of cis-[Ru(bpy)₂L(NO)]ⁿ⁺ Complexes: a Key Role of Physiological Thiols. *J. Inorg. Biochem.* 105, 624–629.
- (24) Holanda, A. K. M., da Silva, F. O. N., Sousa, J. R., Diógenes, I. C. N., Carvalho, I. M. M., Moreira, I. S., Clarke, M. J., and Lopes, L. G. F. (2008) Photochemical NO release from nitrosyl Ru-II complexes with C-bound imidazoles. *Inorg. Chim. Acta* 361, 2929–2933.
- (25) Silva, F. O. N., Araujo, S. X. B., Holanda, A. K. M., Meyer, E., Sales, F. A. M., Diógenes, H. C. N., Carvalho, I. M. M., Moreira, I. S., and Lopes, L. G. F. (2006) Synthesis, characterization, and NO release study of the cis- and trans-[Ru(bpy)₂(SO₃)(NO)]⁺ complexes. *Eur. J. Inorg. Chem.* 2006, 2020–2026.
- (26) Leitao Junior, A. S., Campos, R. M., Cerqueira, J. B., Fonteles, M. C., Santos, C. F., de Nucci, G., Sousa, E. H., Lopes, L. G., Gonzaga-Silva, L. F., and Nascimento, N. R. (2016) Relaxant effect of a metal-based drug in human corpora cavernosa and its mechanism of action. *Int. J. Impotence Res.* 28, 20–24.
- (27) Campelo, M. W. S., Oria, R. B., de Franca Lopes, L. G., Brito, G. A. D., dos Santos, A. A., de Vasconcelos, R. C., da Silva, F. O. N., Nobrega, B. N., Bento-Silva, M. T., and de Vasconcelos, P. R. L. (2012) Preconditioning with a Novel Metallopharmaceutical NO Donor in Anesthetized Rats Subjected to Brain Ischemia/Reperfusion. *Neurochem. Res.* 37, 749–758.
- (28) Silva, J. J., Guedes, P. M., Zottis, A., Balliano, T. L., Nascimento Silva, F. O., Franca Lopes, L. G., Ellena, J., Oliva, G., Andricopulo, A. D., Franco, D. W., and Silva, J. S. (2010) Novel ruthenium complexes as potential drugs for Chagas's disease: enzyme inhibition and in vitro/in vivo trypanocidal activity. *Br. J. Pharmacol.* 160, 260–269.
- (29) Pavanelli, W. R., da Silva, J. J. N., Panis, C., Cunha, T. M., Costa, I. C., de Menezes, M. C. N. D., de Abreu Oliveira, F. J. D., de Franca Lopes, L. G. D., Cecchini, R., de Queiroz Cunha, F. D., Watanabe, M. A. E., and Itano, E. N. (2011) Experimental Chemotherapy in Paracoccidioidomycosis Using Ruthenium NO Donor. *Mycopathologia* 172, 95–107.
- (30) Santana, A. P., Tavares, B. M., Lucetti, L. T., Gouveia, F. S., Jr., Ribeiro, R. A., Soares, P. M., Sousa, E. H., Lopes, L. G., Medeiros, J. V., and Souza, M. H. (2015) The nitric oxide donor cis-[Ru(bpy)₂(SO₃-NO)](PF₆) increases gastric mucosa protection in mice— involvement of the soluble guanylate cyclase/K(ATP) pathway. *Nitric Oxide* 45, 35–42.
- (31) Staurengo-Ferrari, L., Mizokami, S. S., Silva, J. J., da Silva, F. O. N., Sousa, E. H. S., da Franca, L. G., Matuoka, M. L., Georgetti, S. R., Baracat, M. M., Casagrande, R., Pavanelli, W. R., and Verri, W. A. (2013) The ruthenium NO donor, [Ru(bpy)₂(NO)SO₃](PF₆), inhibits inflammatory pain: Involvement of TRPV1 and cGMP/ PKG/ATP-sensitive potassium channel signaling pathway. *Pharmacol. Biochem. Behav.* 105, 157–165.
- (32) Zapata, A. L., Kumar, M. R., Pervitsky, D., and Farmer, P. J. (2013) A singular value decomposition approach for kinetic analysis of reactions of HNO with myoglobin. *J. Inorg. Biochem.* 118, 171–178.
- (33) Miranda, K. M., Nims, R. W., Thomas, D. D., Espey, M. G., Citrin, D., Bartberger, M. D., Paolucci, N., Fukuto, J. M., Feelisch, M., and Wink, D. A. (2003) Comparison of the reactivity of nitric oxide and nitroxyl with heme proteins. A chemical discussion of the differential biological effects of these redox related products of NOS. *J. Inorg. Biochem.* 93, 52–60.
- (34) Bazylinski, D. A., and Hollocher, T. C. (1985) Metmyoglobin and Methemoglobin as Efficient Traps for Nitrosyl Hydride (Nitroxyl) in Neutral Aqueous-Solution. *J. Am. Chem. Soc.* 107, 7982–7986.
- (35) Cooper, C. E. (1999) Nitric oxide and iron proteins. *Biochim. Biophys. Acta, Bioenerg.* 1411, 290–309.
- (36) Sharma, V. S., Isaacson, R. A., John, M. E., Waterman, M. R., and Chevon, M. (1983) Reaction of nitric oxide with heme proteins: studies on metmyoglobin, opossum methemoglobin, and microperoxidase. *Biochemistry* 22, 3897–3902.
- (37) Akaike, T., Yoshida, M., Miyamoto, Y., Sato, K., Kohno, M., Sasamoto, K., Miyazaki, K., Ueda, S., and Maeda, H. (1993) Antagonistic Action of Imidazolineoxyl N-Oxides against Endothelium-Derived Relaxing Factor.No through a Radical Reaction. *Biochemistry* 32, 827–832.
- (38) Bobko, A. A., Bagryanskaya, E. G., Reznikov, V. A., Kolosova, N. G., Clanton, T. L., and Khramtsov, V. V. (2004) Redox-sensitive mechanism of no scavenging by nitronyl nitroxides. *Free Radical Biol. Med.* 36, 248–258.
- (39) Bobko, A. A., Ivanov, A., and Khramtsov, V. V. (2013) Discriminative EPR detection of NO and HNO by encapsulated nitronyl nitroxides. *Free Radical Res.* 47, 74–81.
- (40) Samuni, U., Samuni, Y., and Goldstein, S. (2010) On the Distinction between Nitroxyl and Nitric Oxide Using Nitronyl Nitroxides. *J. Am. Chem. Soc.* 132, 8428–8432.
- (41) Donzelli, S., Espey, M. G., Thomas, D. D., Mancardi, D., Tocchetti, C. G., Ridnour, L. A., Paolucci, N., King, S. B., Miranda, K. M., Lazzarino, G., Fukuto, J. M., and Wink, D. A. (2006) Discriminating formation of HNO from other reactive nitrogen oxide species. *Free Radical Biol. Med.* 40, 1056–1066.
- (42) Gama Sawaia, M. G., and Santana da Silva, R. S. (2003) The reactivity of nitrosyl ruthenium complexes containing polypyridyl ligands. *Transition Met. Chem.* 28, 254–259.
- (43) Masoud, G. N., and Li, W. (2015) HIF-1alpha pathway: role, regulation and intervention for cancer therapy. *Acta Pharm. Sin. B* 5, 378–389.
- (44) Kallio, P. J., Wilson, W. J., O'Brien, S., Makino, Y., and Poellinger, L. (1999) Regulation of the hypoxia-inducible transcription factor 1alpha by the ubiquitin-proteasome pathway. *J. Biol. Chem.* 274, 6519–6525.
- (45) Salceda, S., and Caro, J. (1997) Hypoxia-inducible factor 1alpha (HIF-1alpha) protein is rapidly degraded by the ubiquitin-proteasome system under normoxic conditions. Its stabilization by hypoxia depends on redox-induced changes. *J. Biol. Chem.* 272, 22642–22647.
- (46) Metzen, E., Zhou, J., Jelkmann, W., Fandrey, J., and Brune, B. (2003) Nitric oxide impairs normoxic degradation of HIF-1alpha by inhibition of prolyl hydroxylases. *Mol. Biol. Cell* 14, 3470–3481.
- (47) Chowdhury, R., Godoy, L. C., Thiantanawat, A., Trudel, L. J., Deen, W. M., and Wogan, G. N. (2012) Nitric oxide produced endogenously is responsible for hypoxia-induced HIF-1alpha stabilization in colon carcinoma cells. *Chem. Res. Toxicol.* 25, 2194–2202.
- (48) Sun, H. L., Liu, Y. N., Huang, Y. T., Pan, S. L., Huang, D. Y., Guh, J. H., Lee, F. Y., Kuo, S. C., and Teng, C. M. (2007) YC-1 inhibits HIF-1 expression in prostate cancer cells: contribution of Akt/NF-kappaB signaling to HIF-1alpha accumulation during hypoxia. *Oncogene* 26, 3941–3951.
- (49) Pereira, J. C. M., Souza, M. L., and Franco, D. W. (2015) Nitric Oxide and Nitroxyl Products from the Reaction of L-Cysteine with

trans-[RuNO(NH₃)(4)P(OEt)(3)](PF₆)(3). *Eur. J. Inorg. Chem.* 2015, 1005–1011.

(50) Montenegro, A. C., Bari, S. E., and Olabe, J. A. (2013) Reactivity of iron(II)-bound nitrosyl hydride (HNO, nitroxyl) in aqueous solution. *J. Inorg. Biochem.* 118, 108–114.

(51) Salie, M. J., Oram, D. S., Kuipers, D. P., Scripture, J. P., Chenge, J., MacDonald, G. J., and Louters, L. L. (2012) Nitroxyl (HNO) acutely activates the glucose uptake activity of GLUT1. *Biochimie* 94, 864–869.

(52) Yang, Y., Sun, M., Wang, L., and Jiao, B. (2013) HIFs, angiogenesis, and cancer. *J. Cell. Biochem.* 114, 967–974.

(53) Glynn, S. A., Boersma, B. J., Dorsey, T. H., Yi, M., Yfantis, H. G., Ridnour, L. A., Martin, D. N., Switzer, C. H., Hudson, R. S., Wink, D. A., Lee, D. H., Stephens, R. M., and Ambs, S. (2010) Increased NOS2 predicts poor survival in estrogen receptor-negative breast cancer patients. *J. Clin. Invest.* 120, 3843–3854.

(54) Proding, W., and Svoboda, O. (1953) Nachweis und Bestimmung von Hydroxylamin mit 8-Oxy-chinolin. *Microchim. Acta* 41, 426–433.

(55) Arnel, D. R., and Stamler, J. S. (1995) NO⁺, NO, and NO-Donation by S-Nitrosothiols - Implications for Regulation of Physiological Functions by S-Nitrosylation and Acceleration of Disulfide Formation. *Arch. Biochem. Biophys.* 318, 279–285.

(56) Beccano-Kelly, D. A., Kuhlmann, N., Tatarnikov, I., Volta, M., Munsie, L. N., Chou, P., Cao, L. P., Han, H., Tapia, L., Farrer, M. J., and Milnerwood, A. J. (2014) Synaptic function is modulated by LRRK2 and glutamate release is increased in cortical neurons of G2019S LRRK2 knock-in mice. *Front. Cell. Neurosci.* 8, 301–311.

■ NOTE ADDED AFTER ASAP PUBLICATION

This paper was published on May 31, 2016. Figure 5 has been updated and the revised version was posted on June 2, 2016.